atmosphere

MDPI

Article

Multiple Factors Driving Carbonate System in Subtropical Coral Community Environments along Dapeng Peninsula, South China Sea

Bo Yang [1,2], Zhuo Zhang [3], Zhouping Cui [1], Ziqiang Xie [1], Bogui Chen [1], Huina Zheng [1,4], Baolin Liao [1], Jin Zhou [2,*] and Baohua Xiao [1,3,*]

[1] Shenzhen Institute of Guangdong Ocean University, Binhai 2 Road, Shenzhen 518120, China
[2] Shenzhen International Graduate School, Tsinghua University, Shenzhen 518055, China
[3] College of Fisheries, Guangdong Ocean University, Zhanjiang 524088, China
[4] College of Food Science and Technology, Guangdong Ocean University, Zhanjiang 524088, China
* Correspondence: zhou.jin@sz.tsinghua.edu.cn (J.Z.); xiaobh@gdou.edu.cn (B.X.)

Abstract: Coral reef ecosystems have extremely high primary productivity and play an important role in the marine carbon cycle. However, due to the high carbon metabolism efficiency of coral communities, little is known about the carbon sink–source properties of coral reefs. In November 2022, in situ field investigations coupled with incubation experiments were conducted in typical subtropical coral reef waters, i.e., Yangmeikeng Sea Area (Area I) and Dalu Bay (Area II), to explore the dynamics of the carbonate system and its controlling factors. The results revealed that the carbonate parameters had high variability, comprehensively forced by various physical and biochemical processes. Overall, Areas I and II were net sinks of atmospheric CO_2, with net uptake fluxes of 1.66 ± 0.40 and 0.99 ± 0.08 mmol C m^{-2} day^{-1}, respectively. The aragonite saturation state (Ω_A), 3.04–3.87, was within the range adequate for growth of tropical shallow-water scleractinian corals. Inorganic carbon budget results indicated that photosynthesis and microbial respiration were the main factors affecting the dynamics of carbonate systems in the whole study area. However, focusing on the reef areas, coral metabolism was also a key factor affecting the carbonate system in seawater (especially in Area I) and its contribution accounted for 28.9–153.3% of the microbial respiration. This study highlighted that metabolism of coral communities could significantly affect the seawater carbonate system, which is of great significance in the context of the current process of ocean acidification.

Keywords: coral community environment; carbonate system; coral metabolism; photosynthesis; microbial respiration

Citation: Yang, B.; Zhang, Z.; Cui, Z.; Xie, Z.; Chen, B.; Zheng, H.; Liao, B.; Zhou, J.; Xiao, B. Multiple Factors Driving Carbonate System in Subtropical Coral Community Environments along Dapeng Peninsula, South China Sea. *Atmosphere* **2023**, *14*, 688. https://doi.org/10.3390/atmos14040688

Academic Editors: Peng Zhang, Chuancheng Fu and Jian Liu

Received: 16 January 2023
Revised: 2 April 2023
Accepted: 4 April 2023
Published: 6 April 2023

1. Introduction

Driven mainly by anthropogenic activity, e.g., the burning of fossil fuels and changes in land use, the atmospheric carbon dioxide (CO_2) concentration has increased by ~45% since the Industrial Revolution, from 280 ppm to more than 410 ppm in 2022 [1]. As the world's largest carbon reservoir, the ocean has absorbed ~30% of the anthropogenic CO_2, which has altered the marine carbonate system. For example, the pH of global surface ocean has decreased by ~0.1 units, and the aragonite saturation state (Ω_A) has decreased by roughly 0.5 units [2–5]. This significant change in marine chemistry has a serious impact on marine ecosystems, especially those dominated by calcified organisms, e.g., reef-building corals and shellfish [6,7]. Therefore, it is an important topic for scientists to clarify the key influencing mechanism of the marine inorganic carbon cycle and take effective mitigation measures.

Over the past few decades, the research of CO_2 systems has mainly focused on the ocean and tropical regions [8,9]. In comparison, the inorganic carbon dynamics in coastal waters have received relatively little attention [6,10,11]. Due to multiple pressures from

nature and human activities, e.g., input of nutrients and organic pollutants, the carbon cycle in coastal waters is more active, and the dynamics of CO_2 systems are usually more complex [6,12]. On a global scale, coastal waters have generally been the sinks of atmospheric CO_2 with a net absorption of ~20 Tmol C yr^{-1} [13,14]. However, these CO_2 sink/source properties vary both spatially and temporally, and are mainly driven by differences in physical and biochemical factors [15–17]. For example, high latitude and temperate bodies of water generally act as atmospheric CO_2 sinks, while subtropical and tropical waters act as atmospheric CO_2 sources. Even in the same coastal waters, the near-shore areas may act as atmospheric CO_2 sources, but the offshore zones may act as CO_2 sinks [14,15].

For the control process of the carbonate system, it is well known that the carbon metabolism of marine communities, that is, the balance of photosynthesis and respiration, is considered to be the be key factor [18–23]. Generally, in a net autotrophic ecosystem where photosynthesis is greater than respiration, the uptake of CO_2 by photosynthesis exceeds it produced by mineralization, which increases pH, carbonate ion concentration (CO_3^{2-}) and Ω_A, and decreases dissolved inorganic carbon (DIC) and partial pressure of CO_2 (pCO_2). In addition, due to the formation and metabolism of biogenic calcium carbonate ($CaCO_3$), calcified communities also have important effects on the dynamics of the carbonate system in coastal waters, especially in those areas with a large number of calcified organisms, e.g., coral reefs and shellfish breeding areas [24–27]. Generally, biocalcification can absorb total alkalinity (TAlk) and DIC from seawater in a 2:1 stoichiometric ratio [28], resulting in an overall increase in seawater pCO_2, thus forming a net CO_2 source effect [29].

In addition, environmental factors such as temperature and hydrodynamics can affect the dynamics of a carbonate system in coastal waters [6]. For example, increasing temperature can reduce CO_2 solubility in seawater. Meanwhile, temperature can significantly affect the metabolic process of marine organisms, such as photosynthesis, respiration and calcification, thereby regulating the CO_2 source and sink attributes of the system [6,19–21]. Hydrodynamic processes affect the carbonate system by driving the mixing of different water masses. For example, the mixing of land-derived freshwater (with low DIC concentration) and seawater (with high DIC concentration) make a relatively large contribution to the CO_2 system in the northern East China Sea [30] and Yellow Seas of China [31].

The coral reef ecosystem has extremely high primary productivity and plays an important role in the marine carbon cycle. Meanwhile, as the main calcified community system, coral reefs contribute up to 7–15% of global marine $CaCO_3$ production [32]. Therefore, the carbon metabolism process of coral communities may significantly affect the coastal carbonate system. Previous studies have indicated that coral reefs typically act as the source of atmospheric CO_2, releasing 0.005 to 0.08 Gt C as CO_2 annually, with an average emission of 1.51 mol C m^{-2} yr^{-1} [33]. However, it should be emphasized that these above CO_2 fluxes were obtained based on a few ecosystems. In addition, the organic carbon (OC) metabolic processes of coral communities, reef organisms and microorganisms can also significantly affect the concentration of TAlk and DIC in waters, thereby altering the carbonate system in the entire coral reef area [34]. Therefore, the balance between production/metabolism of OC and $CaCO_3$ controls the CO_2 budget in the coral reef ecosystem [32]. However, the final outcome of the above process is also controlled by various factors, such as coral species and health status, and hydrological conditions in coral reef waters [22,29]. Under different conditions, the sink–source properties of CO_2 in coral reefs may be significantly different, which requires further study.

The South China Sea (SCS) with hundreds of coral reefs is an active area of marine carbon cycle. Previous studies indicated that the coral reefs in this area mostly act as a source of atmospheric CO_2 [35,36]. However, as far as we know, the above results are mainly based on the analysis of tropical coral reefs. Little is known about the carbonate system dominated by subtropical coral reefs, where the environmental characteristics are significantly different from those in tropical coral reefs. The coastal waters of Dapeng Peninsula, located in the SCS next to the eastern coastline of Shenzhen, belong to subtropical waters, and have a

large number of coral colonies distributed throughout [37–39]. The metabolic processes of these corals and related organisms may significantly affect the dynamics of the carbonate system in seawater, but the relevant information is still unknown. Thus, in November 2022, the carbonate systems were investigated in the Yangmeikeng Sea Area (Area I) and Dalu Bay (Area II), two typical subtropical coral community environments along Dapeng Peninsula. The main objectives were (1) to determine the behavior of inorganic carbon chemistry in the coral community environment in Areas I and II, and (2) to reveal their main control processes.

2. Materials and Methods

2.1. Study Area and Field Sampling

The research areas located in the coastal waters of Dapeng Peninsula are important habitats for scleractinian coral communities in China with a total coral distribution area of ~200 hectares. The scleractinian corals are widely distributed in Area I, with an area of ~93 hectares; in contrast, the corals in Area II are only distributed along the coast, with a total area of ~6 hectares. The dominant species are *Acropora pruinose, Porites lutea, Favia favus, Acropora digitifera* and *Platygyra carnosus*. The water depth is mostly ~15 m and the water temperature ranges from 15 to 31 °C [40–42]. There are no large rivers along the coast of the study area, only a small river, i.e., Yangmei River, discharging into Area I. In November 2022, a total 31 stations were investigated in Areas I and II for eco-environmental and carbonate information (Figure 1). Water samples were collected from surface and bottom layers.

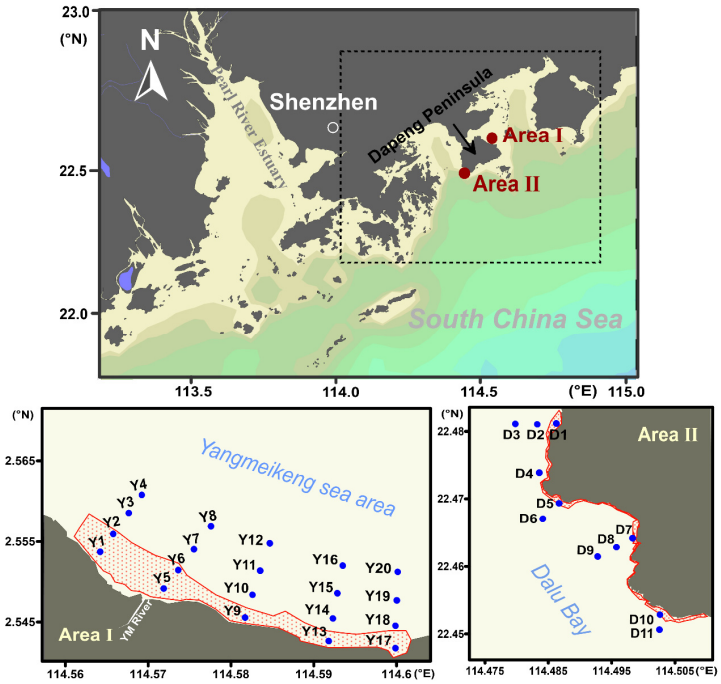

Figure 1. Sampling sites in the coastal waters near Dapeng Peninsula, South China Sea. Areas I and II are located in the Yangmeikeng sea area (Area I) and Dalu Bay (Area II), respectively. YM River represents the Yangmei River. The red area in the figure indicates the coral reef area.

2.2. Analytical Methods

Environmental parameters, including temperature, salinity, DO and chlorophyll *a* (Chl *a*), were measured via YSI sensors with the corresponding precisions of ± 0.05 °C, ± 0.01, ± 0.3 μmol L^{-1} and 0.01 μg L^{-1}, respectively. During the investigation period, the methods of Winkler titration and ultraviolet spectrophotometer were used to correct the DO and Chl *a* data obtained via YSI sensors [6,43]. In addition, apparent oxygen utilization (AOU), an indicator of net biological metabolism, was obtained by subtracting the DO

measured on site from the air-equilibrated DO [44]. Primary productivity, expressed as *PP*, was calculated according to the formula $PP = C_{\text{chl a}} \times Q \times E \times D/2$ [45]. In the above formula, $C_{\text{chl a}}$ represents the Chl *a* concentration (μg L^{-1}), *Q* is the assimilation coefficient (3.7) [46,47], and *E* and *D* represent the depth of the true light layer (m) and duration of sunlight (h), respectively.

pH_T was measured in situ via a pH meter equipped with a Metter Toledo pH Electrode with an accuracy of ± 0.001 pH unit. Water samples for TAlk and DIC analyses were collected in 100 mL and 50 mL borosilicate glass bottles and fixed with 30 μL saturated $HgCl_2$ solutions. After returning to the laboratory, water samples were placed in a thermostat water bath at 25 °C for 12 h before the measurements of TAlk and DIC. TAlk and DIC were determined using a Metter Toledo titrator (G10S) and an Apollo inorganic carbon analyzer [6,48]. The measurement precisions were assessed to be ±2 μmol kg^{-1} for DIC and ±3 μmol kg^{-1} for TAlk based on the determination of certificated DIC and TAlk reference from A.G. Dickson's lab (Batch 144).

Other carbonate parameters, including pCO_2, Ω_A and pH_T at in situ ($pCO_{2@\text{ in situ}}$, $\Omega_{A@\text{ in situ}}$ and $pH_{T@\text{ in situ}}$) and average temperature ($pCO_{2@\,23.7\,^\circ C}$, $\Omega_{A@\,23.7\,^\circ C}$ and $pH_{T@\,23.7\,^\circ C}$) during the investigation period were calculated from TAlk, DIC, temperature and salinity using the calculation program CO2SYS software [49]. $pCO_{2@\,23.7\,^\circ C}$, $\Omega_{A@\,23.7\,^\circ C}$ and $pH_{T@\,23.7\,^\circ C}$ remove the direct thermodynamic temperature effect [19]. In the above calculation process, the dissociation constants for carbonic acid (K1 and K2), potassium bisulfate ($KHSO_4$) and boron-to-chlorinity ratio were obtained from the reports in Lueker et al. [50], Dickson [45] and Lee et al. [51], respectively.

2.3. Laboratory Incubation Experiments

2.3.1. Microbial Respiration in Seawater

In order to determine the effect of microbial respiration on the carbonate system in seawater, six representative stations, i.e., Y5, Y6, Y7, D5, D6 and D8 (Figure 1), were selected for incubation experiments, and the specific method was that of Yang et al. [6,27]. Briefly, ~2 L unfiltered seawater was filled into two 1 L culture bottles. Into one bottle was added 1 mL saturated mercury chloride solution as the control group, and the other bottle was left without any treatment. All culture bottles were sealed with no headspace and transferred to an incubator for dark incubation. The experiments were conducted for 48 h at 23.7 ± 0.5 °C (average temperature of the study area during the investigation period) for 48 h. The concentration of TAlk and DIC in the bottles was determined at 0, 12, 24 and 48 h, respectively. The DIC production rate ($P_{\text{M-DIC}}$, μmol kg^{-1} day^{-1}) and TAlk consumption rate ($C_{\text{M-TAlk}}$, μmol kg^{-1} day^{-1}) by microbial respiration was calculated as follows:

$$P_{\text{M-DIC}} = (k_0 - k) \times 24$$

$$C_{\text{M-TAlk}} = (k_0 - k) \times 244$$

where k_0 and k are the linear regression slopes of DIC or TAlk (μmol kg^{-1}) vs. time (h) in the control and sample groups, respectively.

2.3.2. Coral Metabolism

Similarly, incubation experiments were conducted to study the effects of coral metabolism on the carbonate system by analyzing the changes in TAlk and DIC in seawater. The corals used in the experiments (*Acropora pruinose, Porites lutea, Favia favus, Acropora digitifera* and *Platygyra carnosus*) were collected in Areas I and II. The collected corals were brought back to the laboratory within 2 h. Meanwhile, 10 L seawater was collected on site and filtered through GF/F filters for subsequent coral incubation experiments.

After reaching the laboratory, replicate specimens from separate corals were quickly transferred to 1 L glass bottles filled with exactly 900 mL of filtered seawater. In addition, three bottles in which only filtered seawater was added were selected as the control group. All culture bottles were sealed without headspace and moved to a biochemical incubator

for 48 h (with 12 h light/12 h dark cycle), and experimental temperatures were set to 23.7 ± 0.5 °C. TAlk and DIC concentration in the bottles was determined at 0, 24 and 48 h during the experiments. The DIC production rate ($P_{C\text{-}DIC}$, μmol cm^{-2} day^{-1}) and TAlk consumption rate ($C_{C\text{-}TAlk}$, μmol cm^{-2} day^{-1}) by coral metabolism were calculated as follows:

$$P_{C\text{-}DIC} = (DIC_1 - DIC_0) \times V \times \rho/(S \times t) \times 24$$

$$C_{C\text{-}TAlk} = (TAlk_1 - TAlk_0) \times V \times \rho/(S \times t) \times 24$$

where DIC_0 ($TAlk_0$) and DIC_1 ($TAlk_1$) are the initial and final DIC (TAlk) concentration (μmol kg^{-1}) of the experiment, respectively, V is the experimental water volume (L), ρ (kg m^{-3}) is the density of seawater, t is the experiment time (h) and S is the surface area of coral branches (cm^{-2}), which is obtained via the aluminum foil technology method [52].

2.4. Estimation of CO_2 Fluxes

The uptake/release fluxes of CO_2 (FCO_2, mmol m^{-2} day^{-1}) were calculated based on the difference between partial pressure of sea surface CO_2 ($pCO_{2\text{-}sea}$) and atmosphere ($pCO_{2\text{-}air}$) according to the formula:

$$FCO_2 = k \times K_0 \times (pCO_{2\text{-}sea} - pCO_{2\text{-}air})$$

where K_0 and k (cm h^{-1}) represent solubility coefficient and transfer velocity of CO_2 [53]. Here, we use 414.71 μatm as the $pCO_{2\text{-}air}$, which was the average concentration of global atmospheric CO_2 in 2021 [1]. k was obtained according to the equation of Wanninkhof [54] as follows:

$$k = 0.27 \times {u_{10}}^2 \times (Sc/660)^{-0.5}$$

where Sc and u_{10} (m s^{-1}) represent the Schmidt number in seawater and wind speed at 10 m above the sea surface [54]. In this study, the u_{10} data were obtained from the South China Sea and the Adjacent Seas Data Center [55].

3. Results

3.1. Environmental Variables

During the investigation periods, water mass was vertically mixed evenly (Figure A1). Temperature and salinity in Areas I and II were relatively stable, ranging from 23.0 to 25.2 °C and 31.0 to 32.8, respectively (Figure A1a). High temperature generally occurred in the near-shore areas, which was contrary to the distribution of salinity (Figures A2 and A3).

The DO in water showed high concentration, 6.66–10.04 mg L^{-1}, and most of them reached saturation (Figure A1b). Spatially, the distribution of surface DO in Area I was higher in the west zone than that in the east area, while the surface DO in Area II was relatively uniform. Different from those in the surface water, the high DO values in the bottom water were mainly distributed in the inshore areas in Areas I and II, which was consistent with the distribution of temperature (Figures A2 and A3).

The Chl *a* concentration varied considerably during the study period, especially in Area I (1.28–23.42 μg L^{-1}) with the high values mainly occurring in the samples of 1–2 m below the water surface. In comparison, the Chl *a* concentration, 0.79–3.79 μg L^{-1}, in Area II was relatively stable (Figure A1c). Consistent with DO, the high values of Chl *a* in the bottom water were mainly distributed in the inshore areas. As shown in Figures A2 and A3, the spatial distribution of Chl *a* was almost consistent with that of DO in Areas I and II.

3.2. Carbonate Parameters in Yangmeikeng Sea Area and Dalu Bay

3.2.1. Yangmeikeng Sea Area (Area I)

The TAlk values ranged from 1976.7 to 2221.6 μmol kg^{-1} with mean values of 2167.3 ± 49.6 and 2181.3 ± 12.5 μmol kg^{-1} in the surface and bottom water. Correspondingly, the DIC values ranged from 1655.3 to 1935.7 μmol kg^{-1} with averages of 1898.7 ± 55.4 μmol kg^{-1} (surface) and 1887.2 ± 18.4 μmol kg^{-1} (bottom). Spatially, the low values of TAlk and DIC in the surface

water mainly appeared at the mouth of Yangmei River (Figure 1), highlighting the impact of river input. However, no obvious spatial distribution characteristics of TAlk were observed in the bottom water. As for bottom DIC, its concentration in the coral reef area was significantly higher than that in the non-coral reef area ($p < 0.05$, Figure A4). Specifically, the bottom DIC in the coral reef area was ~10 μmol kg^{-1} higher than that in the non-reef area, indicating the significant effect of coral activity on DIC dynamics (Figure A4).

The $pH_{T@\ in\ situ}$ varied from 8.074 to 8.200 with averages of 8.140 ± 0.032 in the surface water and 8.109 ± 0.021 in the bottom water. The surface $pH_{T@\ in\ situ}$ was higher in the west area than that in the east zone, which was consistent with the distribution of Chl *a* and DO (Figures 2 and A2), reflecting the influence of the photosynthetic process of phytoplankton. The distribution of bottom $pH_{T@\ in\ situ}$ was opposite to that of the DIC with low values appearing in the coral reef area, indicating the important role of coral communities (Figure 2). The surface $pCO_{2@\ in\ situ}$ varied from 233.6 to 329.8 μatm with a mean value of 294.1 ± 30.1 μatm. During this period, the Yangmeikeng Sea Area could absorb CO_2 from the atmosphere with FCO_2 values varying from −2.52 to −1.17 mmol C m^{-2} day^{-1} (mean −1.66 ± 0.40 mmol C m^{-2} day^{-1}).

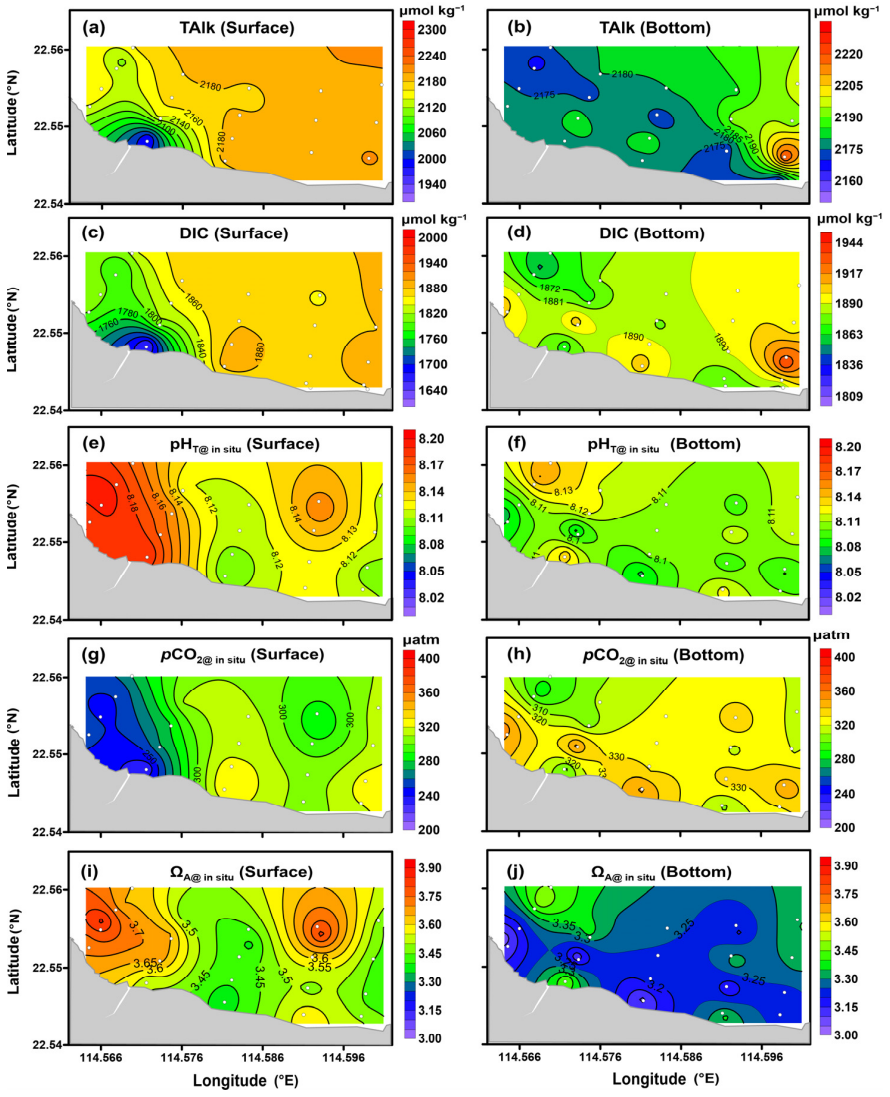

Figure 2. Distribution characteristics of TAlk (**a**,**b**), DIC (**c**,**d**), $pH_{T@\ in\ situ}$ (**e**,**f**), $pCO_{2@\ in\ situ}$ (**g**,**h**) and $\Omega_{A@\ in\ situ}$ (**i**,**j**) in the surface and bottom water of Yangmeikeng Sea Area (Area I).

In the bottom water, the $pCO_{2@\ in\ situ}$ values ranged from 284.4 to 355.6 μatm (mean 323.3 ± 20.0 μatm). Spatially, the surface $pCO_{2@\ in\ situ}$ in the west region was lower than that

in the east area, while the bottom $pCO_{2@\ in\ situ}$ was higher in the near-shore zone than that in the offshore area, which was contrary to that of $pH_{T@\ in\ situ}$ (Figure 2). For the absorption flux of CO_2, the highest value was observed at the Yangmei River mouth (station Y5), while low values were found in the coral reef and adjacent areas, e.g., stations Y9, Y10, Y17 and Y18.

As for $\Omega_{A@\ in\ situ}$, its values ranged from 3.07 to 3.87 with averages of 3.55 ± 0.15 and 3.27 ± 0.12 in the surface and bottom water. Generally, scleractinian corals in the South China Sea require that the Ω_A value should be >2.8 for optimal growth [56]. Thus, the whole study area was conducive to the growth of scleractinian corals in November. Spatially, $\Omega_{A@\ in\ situ}$ was consistent with the distribution of $pH_{T@\ in\ situ}$.

3.2.2. Dalu Bay (Area II)

Comparison with Yangmeikeng Sea Area (Area I), the variations of seawater carbonate parameters were not obvious in Area II (Figures 2 and 3). Overall, there was no significant difference in carbonate parameters (TAlk, DIC, $pH_{T@\ in\ situ}$, $pCO_{2@\ in\ situ}$ and $\Omega_{A@\ in\ situ}$) between the coral reefs and non-reef areas, which was different from the results in Area I. Among them, the TAlk ranged from 2179.1 to 2206.1 μmol kg^{-1} with mean values of 2188.7 ± 7.6 and 2190.0 ± 5.2 μmol kg^{-1} in the surface and bottom water; the corresponding DIC varied from 1887.8 to 1919.5 μmol kg^{-1} (mean 1898.7 ± 8.3 and 1902.9 ± 5.7 μmol kg^{-1}), respectively. Spatially, the concentrations of surface TAlk and DIC were lower in the near-shore area than the offshore area, and were consistent with the distribution of salinity and contrary to the temperature (Figures 3 and A3), while the bottom TAlk did not show obvious spatial variation characteristics (Figure 3).

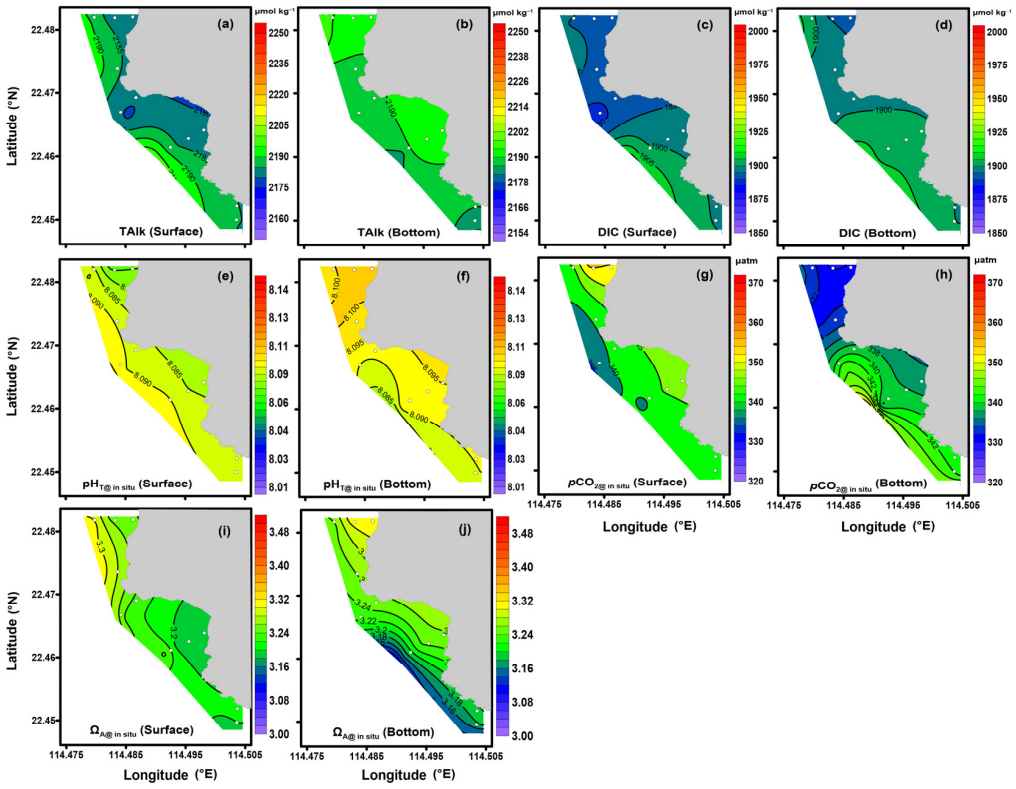

Figure 3. Distribution characteristics of TAlk (**a**,**b**), DIC (**c**,**d**), $pH_{T@\ in\ situ}$ (**e**,**f**), $pCO_{2@\ in\ situ}$ (**g**,**h**) and $\Omega_{A@\ in\ situ}$ (**i**,**j**) in the surface and bottom water of Dalu Bay (Area II).

$pH_{T@\ in\ situ}$ varied from 8.070 to 8.102 with mean values of 8.089 ± 0.007 in the surface water and 8.092 ± 0.009 in the bottom water. The surface $pH_{T@\ in\ situ}$ showed distribution characteristics in the near-shore area lower than the far-shore zone, while the bottom $pH_{T@\ in\ situ}$ showed the opposite distribution characteristics, which was opposite to the

temperature distribution (Figures 3 and A3). $pCO_{2\ @\ in\ situ}$ varied from 329.8 to 360.5 µatm with mean values of 341.7 ± 6.4 and 339.7 ± 8.6 µatm in the surface and bottom water. The distribution of $pCO_{2@\ in\ situ}$ was opposite to that of $pH_{T@\ in\ situ}$ (Figure 3). Similarly, Dalu Bay was a sink of atmospheric CO_2, with FCO_2 values varying from −1.15 to −0.81 mmol C m^{-2} day^{-1} (mean −0.99 ± 0.08 mmol C m^{-2} day^{-1}). In comparison, the CO_2 sink effect in Dalu Bay (Area II) was significantly lower than that in the Yangmeikeng Sea Area (Area I). Spatially, the absorption fluxes of CO_2 showed an increasing trend from the near-shore area to the far-shore zone, with the lowest value appearing at station D1 in the coral reef area.

$\Omega_{A@\ in\ situ}$ values ranged from 3.04 to 3.32 with mean values of 3.25 ± 0.05 and 3.20 ± 0.07 in the surface and bottom water, which was conducive to the growth of scleractinian corals. Consistent with the distribution of $pH_{T@\ in\ situ}$, the surface $\Omega_{A@\ in\ situ}$ showed the distribution characteristics of near-shore area lower than far-shore area, which was contrary to that of the bottom water.

3.3. Microbial Respiration

As shown in Figure 4a, the microbial respiration in November can increase the concentration of DIC in water by 3.00 to 5.60 µmol kg^{-1} day^{-1} with averages of 4.28 ± 0.57 and 3.90 ± 1.47 µmol kg^{-1} day^{-1} in Areas I and II, respectively; the corresponding reduction of TAlk in water was 0.48–0.76 µmol kg^{-1} day^{-1} (Figure 4).

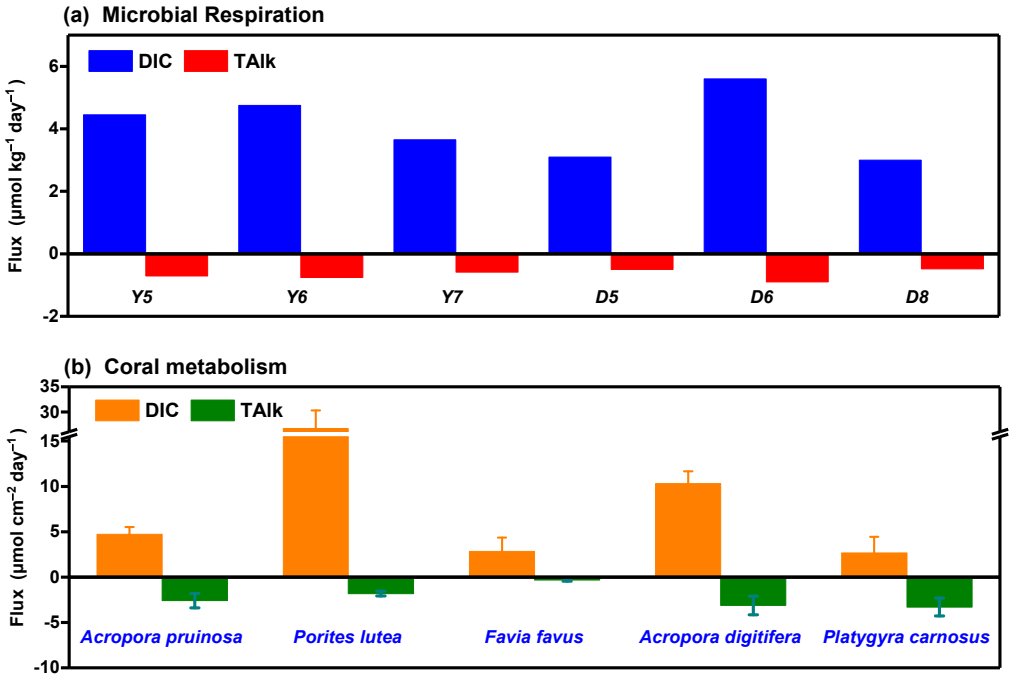

Figure 4. Effects of microbial respiration (**a**) and coral metabolism (**b**) on TAlk and DIC dynamics.

3.4. The Metabolic Processes of Coral Colony

The effect of coral metabolism on the carbonate system is shown in Figure 4b. Daily coral metabolic processes of *Acropora pruinose, Porites lutea, Favia favus, Acropora digitifera* and *Platygyra carnosus* released 4.73 ± 0.78, 23.71 ± 3.63, 2.86 ± 1.49, 10.31 ± 1.36 and 2.67 ± 1.79 µmol cm^{-2} of DIC in seawater, but absorbed 2.60 ± 0.80, 1.81 ± 0.26, 0.32 ± 0.12, 3.12 ± 1.03 and 3.30 ± 0.98 µmol cm^{-2} of Talk from seawater (Figure 4).

4. Discussion

4.1. General Characteristics of Carbonate System

Due to the extremely high primary productivity and efficient carbon metabolism rate of coral communities, the source–sink properties of CO_2 in coral reef ecosystems

are still unclear and need further study. In November 2022, the study areas, i.e., Areas I and II, were net sinks of atmospheric CO_2, with net uptake fluxes of 1.66 ± 0.40 and 0.99 ± 0.08 mmol C m^{-2} day^{-1}, respectively. Compared with other coral reef waters, the TAlk and DIC values in the study area were slightly lower than most of the reef areas listed in Table A1, e.g., Pedra da Risca do Meio Coral Reef [25], Great Barrier Reef [14], Trawler Reef [26], Yongle Atoll [57] and Luhuitou fringing reef [58], while they were higher than those in the reef flat in Northeastern Brazil [59]. Because the values of pH_T, pCO_2 and Ω_A are greatly affected by seasonal temperature changes, these parameters are not compared with the results of other coral reef sea areas. In addition, as described in Section 3.2, the seawater carbonate parameters in the study area, especially in Area I, showed obvious spatial differences, which was comprehensively forced by the physical, e.g., air–sea exchange, and biogeochemical processes (photosynthesis, respiration and calcification) [6,27], and will be discussed in the following sections.

4.2. The Physical Factors Affecting the Carbonate System

4.2.1. Temperature

As shown in Figure 5, temperature was significantly negatively correlated with DIC ($p < 0.05$, $n = 40$) and $pCO_{2\,@\,in\,situ}$ ($p < 0.05$, $n = 40$), but positively correlated with $pH_{T\,@\,in\,situ}$ ($p < 0.05$, $n = 40$) and $\Omega_{A\,@\,in\,situ}$ ($p < 0.01$, $n = 40$) in Area I. This indicated that temperature played an important role in the spatial variation of carbonate parameters [6], which explained 11–48% of their variability (Figure 5A). Similarly, temperature also showed a significant negative correlation with DIC ($p < 0.05$, $n = 22$), but a positive correlation with $\Omega_{A\,@\,in\,situ}$ ($p < 0.01$, $n = 22$) in Area II, and their correlation was more significant than that in Area I (Figure 5A), which explained 48% and 60% of DIC and $\Omega_{A\,@\,in\,situ}$ variability. However, $pH_{T\,@\,in\,situ}$ and $pCO_{2\,@\,in\,situ}$ were not significantly correlated with temperature, suggesting the influence of other processes [21,60,61].

In addition, according to the difference in pH_T, Ω_A and pCO_2 between the in situ and average temperature during the investigation period, the influence of temperature (physical process) on the spatial difference of the carbonate system was quantified [6]. The results showed that −0.009 ± 0.006 (0.008 ± 0.001), 7.15 ± 4.28 (−7.27 ± 1.26) μatm and 0.014 ± 0.009 (−0.012 ± 0.002) of pH_T, pCO_2 and Ω_A in the surface (bottom) water were caused by temperature difference in Yangmeikeng Sea Area (Area I), which only explained 1.5–7.1% of their spatial variability; the corresponding variations in Dalu Bay (Area II) were −0.003 ± 0.008 (−0.006 ± 0.004), 2.45 ± 7.07 (−5.84 ± 4.01) μatm and 0.004 ± 0.011 (−0.009 ± 0.006), which explained 1.4–19.0% of their spatial variability (Figure 5).

To summarize, in the study area, temperature controlled the spatial variation of carbonate parameters by affecting the biochemical and physical dissolution process of CO_2. Among them, the role of biological metabolism was stronger than the physical dissolution of CO_2. However, it is difficult to quantify their respective contributions (biochemical and physical dissolution process) due to the weak linear relationship between carbonate parameters and temperature (Figure 5). In addition, it should be emphasized that this study did not clarify the contribution of temperature to the seasonal variation of carbonate parameters due to the fact that only a one-month survey was conducted, and temperature usually plays a key role in the seasonal variation of these parameters [6]. Thus, additional investigations are needed in the future to remedy this deficiency.

4.2.2. Mixing Effect

Mixing can significantly affect the concentration of TAlk and DIC in seawater, thereby regulating the marine carbonate system [62–64]. As a conservative parameter, surface TAlk was significantly and positively correlated with salinity in Area I ($p < 0.001$, $n = 20$; Figure 5B), suggesting water mixing had a significant effect [62]. As shown in Figure 2, the obvious runoff input of Yangmei River during the investigation period further confirmed the above conclusion. Similarly, surface DIC and salinity showed a significant positive correlation ($p < 0.001$, $n = 40$), which can explain 86% of its spatial variation (Figure 5B).

However, no significant correlation was observed between other parameters and salinity, suggesting the influence of other factors, e.g., biological activity [27]. Different from Area I, the linear relationship between carbonate parameters and salinity was not significant in Area II, which was mainly due to the low runoff input along the coast (Figure A2), as well as the influence of coral metabolism and microbial activity [24–26].

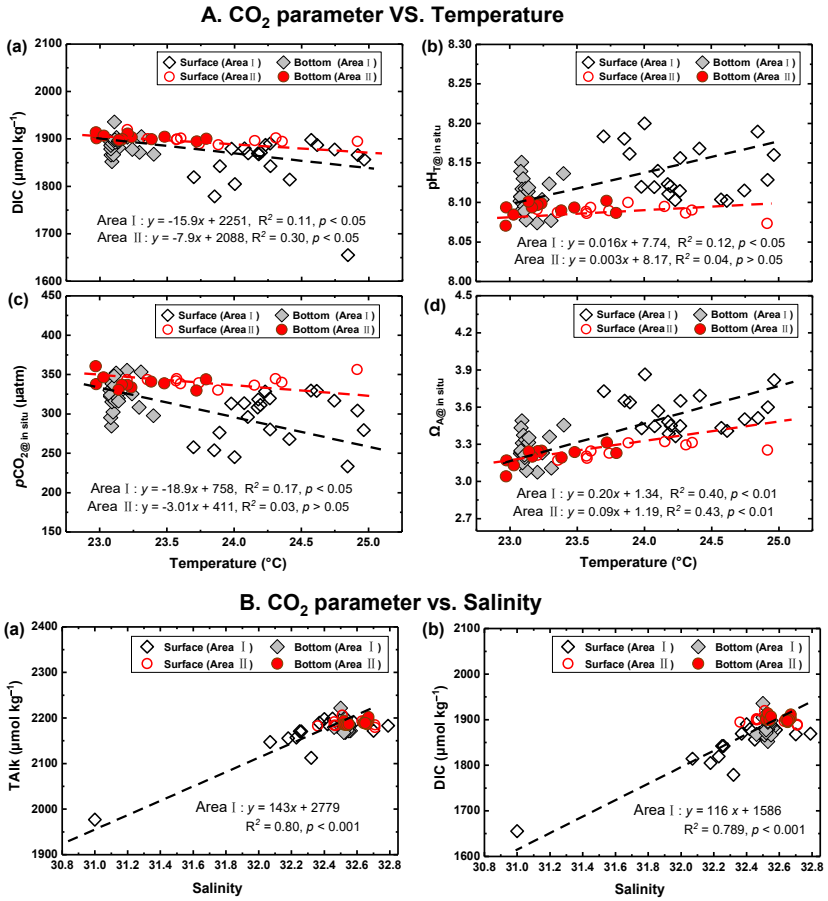

Figure 5. The correlation of inorganic carbon parameters with temperature (**A**) (**a**–**d**) and salinity (**B**) (**a**–**b**) in the surface and bottom water of Yangmeikeng Sea Area (Area I) and Dalu Bay (Area II).

To quantify the effect of the water mixing process on pH_T, pCO_2 and Ω_A, we first normalized the TAlk and DIC according to the average salinity of Area I (32.44) and Area II (32.58), expressed as nTAlk and nDIC [65]; then we calculated $pH_{T\,@\,23.7\,^{\circ}C}$, $pCO_{2\,@\,23.7\,^{\circ}C}$ and $\Omega_{A\,@\,23.7\,^{\circ}C}$ using the CO2SYS program, expressed as $npH_{T\,@\,23.7\,^{\circ}C}$, $npCO_{2\,@\,23.7\,^{\circ}C}$ and $n\Omega_{A\,@\,23.7\,^{\circ}C}$, and finally we calculated the mixing effect based on the difference between the salinity normalized and non-normalized values of the CO_2 parameter [6]. Results indicated that $pH_{T\,@\,23.7\,^{\circ}C}$, $pCO_{2\,@\,23.7\,^{\circ}C}$ and $\Omega_{A\,@\,23.7\,^{\circ}C}$ in the surface (bottom) water changed by 0.009 ± 0.006 (−0.008 ± 0.001), −7.44 ± 4.49 μatm (7.77 ± 1.35 μatm) and −0.03 ± 0.06 (0.02 ± 0.004) due to the mixing effect in Area I. The corresponding changes in Area II were 0.003 ± 0.008 (−0.006 ± 0.004), −2.59 ± 7.11 μatm (5.96 ± 3.89 μatm) and −0.07 ± 0.02 (0.01 ± 0.009), respectively. In other words, on the whole, the mixing effect had little effect on the carbonate system, which only explained ~7.1% (~6.3%), ~6.1% (~6.3%) and ~3.8% (~2.5%) of the spatial difference of pH_T, pCO_2 and Ω_A in the surface (bottom) water in Area I, and ~9.5% (~19.0%), ~8.0% (~19.0%) and ~24.9% (~3.5%) of the spatial difference of pH_T, pCO_2 and Ω_A in the surface (bottom) water in Area II.

4.3. Biological Processes

The relationships between nTAlk and nDIC indicated that photosynthesis, respiration and calcification jointly controlled the dynamics of the carbonate system in Areas I and II (Figure A6). As shown in Figure 6, significant linear correlations between AOU and nDIC, $npH_{T\,@\,23.7\,^{\circ}C}$, $npCO_{2\,@\,23.7\,^{\circ}C}$ and $n\Omega_{A\,@\,23.7\,^{\circ}C}$ were observed in Area I, which indicated that the biological aerobic metabolic activity could be the main process controlling the spatial variations of these CO_2 parameter [66]. As for DIC, the slopes of NDIC-AOU regression, 0.72, were close to the Redfield stoichiometry, i.e., a C/O molar ratio of 0.77 [67], which was similar to those observed in the coastal waters around the Yangma Island [6] and the coast of Mexico [68], indicating that photosynthesis and microbial respiration may be the main processes controlling DIC dynamics [6].

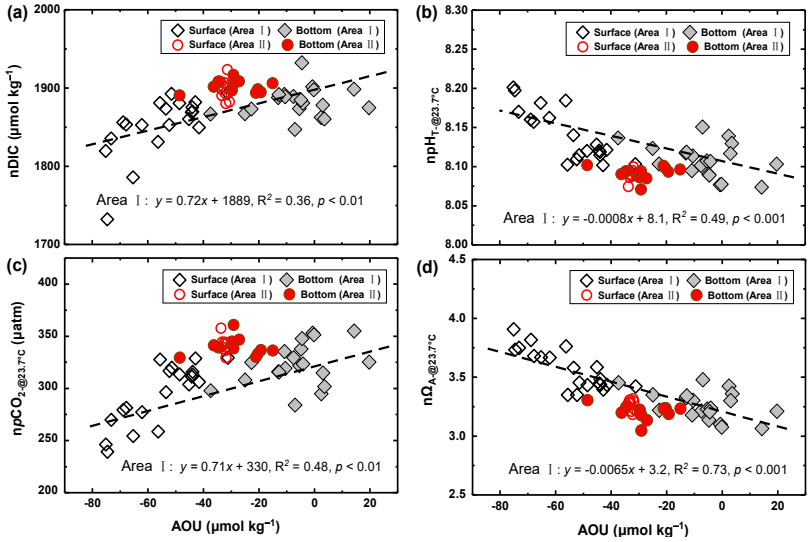

Figure 6. The correlation of inorganic carbon parameters with AOU (**a**–**d**) in the surface and bottom water of Yangmeikeng Sea Area (Area I) and Dalu Bay (Area II).

Generally, photosynthesis can reduce DIC and increase TAlk concentration in seawater at a 106:17 stoichiometric ratio [12,69]. As shown in Figure A7, in the surface water, significant correlations between Chl *a* and the CO_2 parameters, i.e., nDIC, $npH_{T\,@\,23.7\,^{\circ}C}$, $npCO_{2\,@\,23.7\,^{\circ}C}$ and $n\Omega_{A\,@\,23.7\,^{\circ}C}$, were observed in Area I, suggesting photosynthesis plays an important role. However, no significant correlation between carbonate parameters and Chl *a* was found in Area II, indicating other factors interfering in the carbonate system [6].

According to the results of *PP* and mixed layer, the effect of primary production on the CO_2 system was initially quantified. The results indicated that, in Areas I and II, the monthly reduction of DIC in water by primary production were 154.3 ± 104.6 and 69.5 ± 51.7 μmol kg^{-1}, respectively; the corresponding increased TAlk were 24.7 ± 16.8 and 11.1 ± 8.3 μmol kg^{-1}, respectively. Obviously, the impact of primary production on DIC and TAlk in Area I was more significant than that in Area II.

The biological respiration mainly included microbial and coral respiration. Contrary to primary production, biological respiration can increase DIC and reduce TAlk in seawater [12]. The results of incubation experiments showed that, in November, microbial respiration in water increased DIC concentrations by 128.5 ± 17.1 and 117.0 ± 44.2 μmol kg^{-1} in Areas I and II; the corresponding TAlk decreased by 15.8 ± 2.10 and 14.4 ± 5.4 μmol kg^{-1}, respectively. However, it should be noted that for microbial metabolism, we only considered the microbial respiration in water but ignored the related processes in a sedimentary environment, which may underestimate the results of microbial metabolism [70].

The effects of coral metabolic processes on carbonate systems were quantified based on the results of incubation experiments and distribution of corals in Areas I and II (un-

published data). From the perspective of the whole study area, the coral metabolic process in November could increase the DIC concentration of water in Areas I and II by 12.9 and 0.67 μmol kg^{-1}; there was a corresponding decrease in TAlk of 2.90 and 0.15 μmol kg^{-1}, respectively, which was much lower than the contribution of microbial respiration. However, only focusing on the reef area and ignoring the water exchange inside and outside of the reef area, coral communities had a significant impact on the carbonate system, and its metabolic process could increase DIC concentrations of water by 108.0 and 33.8 μmol kg^{-1} in Areas I and II, with a corresponding decrease in TAlk of 24.22 and 7.58 μmol kg^{-1}, respectively. Obviously, coral metabolism in Area I has a more significant effect on carbonate dynamics in the reef area, and its contributions were comparable to that of microbial respiration. In comparison, the coral metabolic process in Area II has a relatively weak effect on the carbonate system, accounting for only 28.9% (DIC) and 52.6% (TAlk) of microbial respiration, respectively.

4.4. Quantification of Processes Controlling the Carbonate System

Biological processes (microbial and coral metabolism) and air–sea exchange can control the dynamics of the carbonate systems in the coral reef area by regulating the concentration of DIC and/or TAlk in the water [14,25,71,72]. In addition, previous research indicated that offshore water intrusion could play a significant role in carbonate dynamics in coastal waters [63]. However, due to lack of up-to-date and reliable relevant data, the impact of this process has not yet been reported. Here, we calculated the effects of photosynthesis, microbial respiration, coral metabolism and air–sea exchange on the carbonate systems in November using the calculation program CO2SYS software based on the changes of TAlk and DIC in the above processes (Figure 7). As shown in Figure 7, from the perspective of the whole of Areas I and II (including reef and non-reef areas), primary production and microbial respiration mainly controlled the dynamics of the carbonate system in November, which was consistent with the results of other coral reef waters, e.g., the Great Barrier Reef [14] and the reef flat in Northeastern Brazil [73]. In comparison, the metabolic process of coral and air–sea exchange of CO_2 had little effect on the carbonate system (Figure 7).

Specifically, in the entirety of Area I, photosynthesis in November increased TAlk, pH_T and Ω_A of seawater by 24.7 μmol kg^{-1}, 0.38 and 1.76, but decreased DIC and pCO_2 by 154.3 μmol kg^{-1} and 541.5 μatm, respectively. In contrast, microbial respiration reduced TAlk, pH_T and Ω_A by 15.8 μmol kg^{-1}, 0.22 and 1.50, and increased DIC and pCO_2 by 128.5 μmol kg^{-1} and 147.6 μatm, respectively (Figure 7). However, coral metabolism and air–sea exchange of CO_2 had little effect on the CO_2 systems. Among them, coral metabolism reduced TAlk, pH_T and Ω_A of seawater by 2.9 μmol kg^{-1}, 0.03 and 0.16, and increased DIC and pCO_2 by 12.9 μmol kg^{-1} and 22.3 μatm, respectively. In comparison, the contribution of coral metabolism to seawater carbonate parameters only accounted for 10–18% of microbial respiration (Figure 7). In addition, the air–sea exchange process in November decreased pH_T and Ω_A in the water by ~0.01 and 0.05, and increased DIC and pCO_2 by 5.0 μmol kg^{-1} and 7.6 μatm, respectively, which accounted for only 3–5% of microbial respiration (Figure 7). In summary, photosynthesis and microbial respiration were the main factors affecting the dynamics of the seawater CO_2 system in the whole of Area I, which were the key processes controlling the CO_2 sink–source properties in this region (Figure 7d).

In comparison, the effect of biochemical processes on the carbonate system in Area II was significantly weaker than that in Area I (Figure 7). Among them, photosynthesis in November only increased TAlk, pH_T and Ω_A of seawater by 11.1 μmol kg^{-1}, 0.15 and 0.81, and decreased DIC and pCO_2 by 69.5 μmol kg^{-1} and 179.0 μatm, respectively, which was 33–46% of the corresponding results in Area I. The microbial respiration results in Area II were comparable to those in Area I, which reduced TAlk, pH_T and Ω_A of seawater by 14.4 μmol kg^{-1}, 0.21 and 1.36, and decreased DIC and pCO_2 by 117.0 μmol kg^{-1} and 154.0 μatm (Figure 7). Consistent with Area I, coral metabolism and air–sea exchange of

CO_2 had little effect on the carbonate system, and their contributions only accounted for <1% and 3–6% of microbial respiration, respectively.

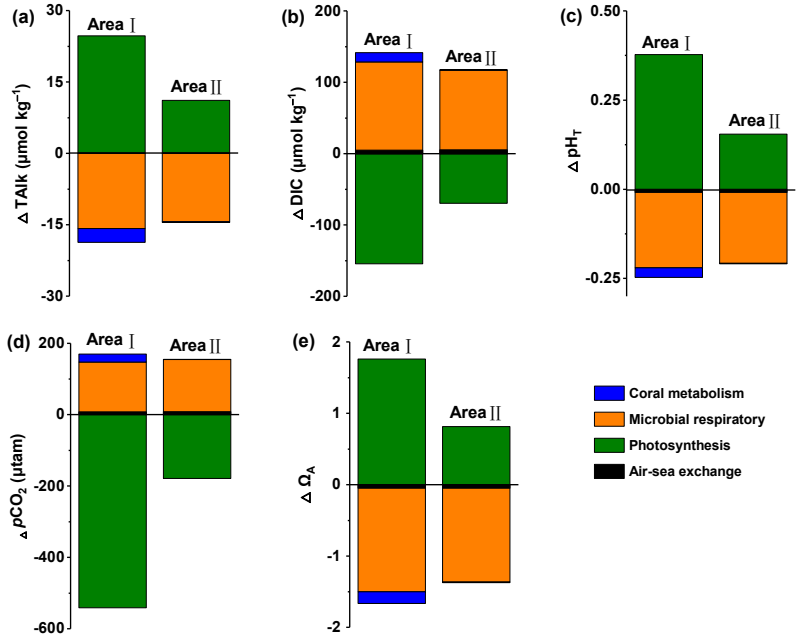

Figure 7. The contribution of photosynthesis, microbial respiration, coral metabolism and air–sea exchange to inorganic carbon dynamics (**a**–**e**) of the entire study area of Yangmeikeng Sea Area (Area I) and Dalu Bay (Area II) in November.

However, it is worth noting that the above results may significantly weaken the role of coral metabolism on the CO_2 system, especially in reef areas [14,68]. As shown in Figure A4, the bottom carbonate parameters of reef and non-reef areas showed significant differences in Area I ($p < 0.05$, $n = 40$), further demonstrating the importance of the role of coral metabolism in reef areas. Thus, to further clarify the effect of coral metabolism, we only focus on the reef area to recalculate the contribution of the photosynthesis, microbial respiration, coral metabolism and air–sea exchange to the inorganic carbon system. It should be noted that the above process ignored the water exchange process between reef and non-reef areas, which may exaggerate the role of coral metabolism to some extent. As shown in Figure A8, in the reef area of Area I, the effect of coral metabolism on the seawater carbonate system in November was almost equivalent to microbial respiration, and its contribution accounted for 84.0–153.3% of microbial respiration (Figure A8). In comparison, coral metabolism had a relatively weak impact on the carbonate system in the reef area of Area II, accounting for only 28.9–52.6% of microbial respiration. Therefore, our results suggested that densely distributed coral communities may significantly affect the inorganic carbon system in seawater, especially under weak hydrodynamic conditions, which may be a key factor in the conversion of reef areas from atmospheric CO_2 sinks to sources.

5. Conclusions

In this study, we clarified the dynamic characteristics and influencing factors of the carbonate system in typical coral community environments along the Dapeng Peninsula in the South China Sea in autumn. The results showed that the whole study area, i.e., Yangmeikeng Sea Area (Area I) and Dalu Bay (Area II) was a net sink of atmospheric CO_2, with corresponding FCO_2 values of -1.66 ± 0.40 and -0.99 ± 0.08 mmol C m^{-2} day^{-1}, respectively. The results of $\Omega_{A\ @\ in\ situ}$, 3.04–3.87, indicated that the environment of Areas I and II was conducive to the growth of corals. Spatially, the inorganic carbon parameters in the study area showed obvious variability, which was driven by multiple factors. From the perspective of the entire study area (including reef and non-reef areas) of Areas I and II,

photosynthesis and microbial respiration were the main factors affecting the dynamics of the carbonate system. Comparatively, coral metabolism, temperature, salinity and air–sea exchange processes had little effect on the carbonate system. However, in coral reef areas, coral metabolism was also a key factor affecting the inorganic carbon system in seawater, and its contribution was almost equivalent to microbial respiration. This means densely distributed coral communities may significantly affect the carbonate systems in seawater, which may be a key factor in the conversion of reef areas from atmospheric CO_2 sinks to sources.

Author Contributions: B.Y.: Investigation, Formal analysis, Writing—original draft. Z.Z. and B.C.: Investigation, Writing. B.X., J.Z. and B.Y.: Conceptualization, Resources, Writing—review & editing. B.X. and B.Y.: Funding acquisition, Writing—review & editing. H.Z., B.L., Z.X. and Z.C.: Writing—review & editing. All authors have read and agreed to the published version of the manuscript.

Funding: This work was financially supported by the Sustainable Development Project of Shenzhen (KCXFZ20211020165547011), General Project of China Postdoctoral Fund (2022M721792), Shenzhen Science and Technology R&D Fund (JCYJ20200109144803833), Guangdong Key Area R & D Program Project (2020B1111030002), Guangdong Basic and Applied Basic Research Foundation (2022A1515110345) and Guangdong Basic and Applied Basic Research Foundation (2023A1515012204).

Institutional Review Board Statement: Not applicable.

Informed Consent Statement: Not applicable.

Data Availability Statement: The data that support the findings of this study are available from the corresponding authors, B. Xiao and J. Zhou, upon reasonable request.

Acknowledgments: Acknowledgement for the data support from South China Sea and Adjacent Seas Data Center, National Earth System Science Data Center, National Science & Technology Infrastructure of China. (http://ocean.geodata.cn/data/dataresource.html, accessed on 25 November 2022).

Conflicts of Interest: The authors declare that they have no known competing financial interests or personal rela-tionships that could have appeared to influence the work reported in this paper.

Appendix A

Table A1. Comparisons in the values of TAlk (μmol kg^{-1}) and DIC (μmol kg^{-1}) from some coral reef waters in the world.

Location	Sampling Time	Talk	DIC	Reference
		(μmol kg^{-1})	**(μmol kg^{-1})**	
Pedra da Risca do Meio Coral Reef	August and November 2020	2325 ± 19	2019 ± 16	Cotovicz et al. [25]
Great Barrier Reef—Australia	September 2009 to August 2016	2288 ± 44	1989 ± 45	Lønborg et al. [14]
Trawler Reef	August 2014	2289.3 ± 4.9	2003.0 ± 19.7	Hannan et al. [26]
Big Vicki's Reef	August 2014	2284.0 ± 9.8	1984.7 ± 14.7	Hannan et al. [26]
Palfrey Reef	August 2014	2278.4 ± 7.4	1981.9 ± 22.7	Hannan et al. [26]
Yongle Atoll, China	July 2013	2776 ± 52	2378 ± 92	Yan et al. [57]
Coral Reef Lagoon Kaneohe Bay —Hawaii	September 2003 to September 2004	2180 ± 36	1920 ± 16	Fagan et al. [71]

Table A1. *Cont.*

Location	Sampling Time	Talk	DIC	Reference
		(μmol kg^{-1})	(μmol kg^{-1})	
The coast of Iriomote Island (Japan)	August 2017	2211 ± 44	1878 ± 103	Akhand et al. [59]
Reef flat in Northeastern Brazil	July 2006	1857.6 ± 42.1	1623.0 ± 39.2	Akhand et al. [59]
	August 2007	2002.3 ± 0.8	1801.1 ± 13.6	Longhini et al. [73]
Luhuitou fringing reef, Sanya Bay, China	July 2010	2312.1 ± 15.3	1994.7 ± 40.9	Zhang et al. [58]
Yongxing Island, China	July to August 2009	2421 ± 142	n.d.	Yan et al. [35]
Fiery Cross Reef, China	July to August 2009	2240 ± 56	n.d.	Yan et al. [35]
Yangmeikeng Sea Area, South China	November 2022	2174.3 ± 36.4	1867.6 ± 33.5	In this study
Dalu Bay		2189.3 ± 6.4	1900.8 ± 10.4	

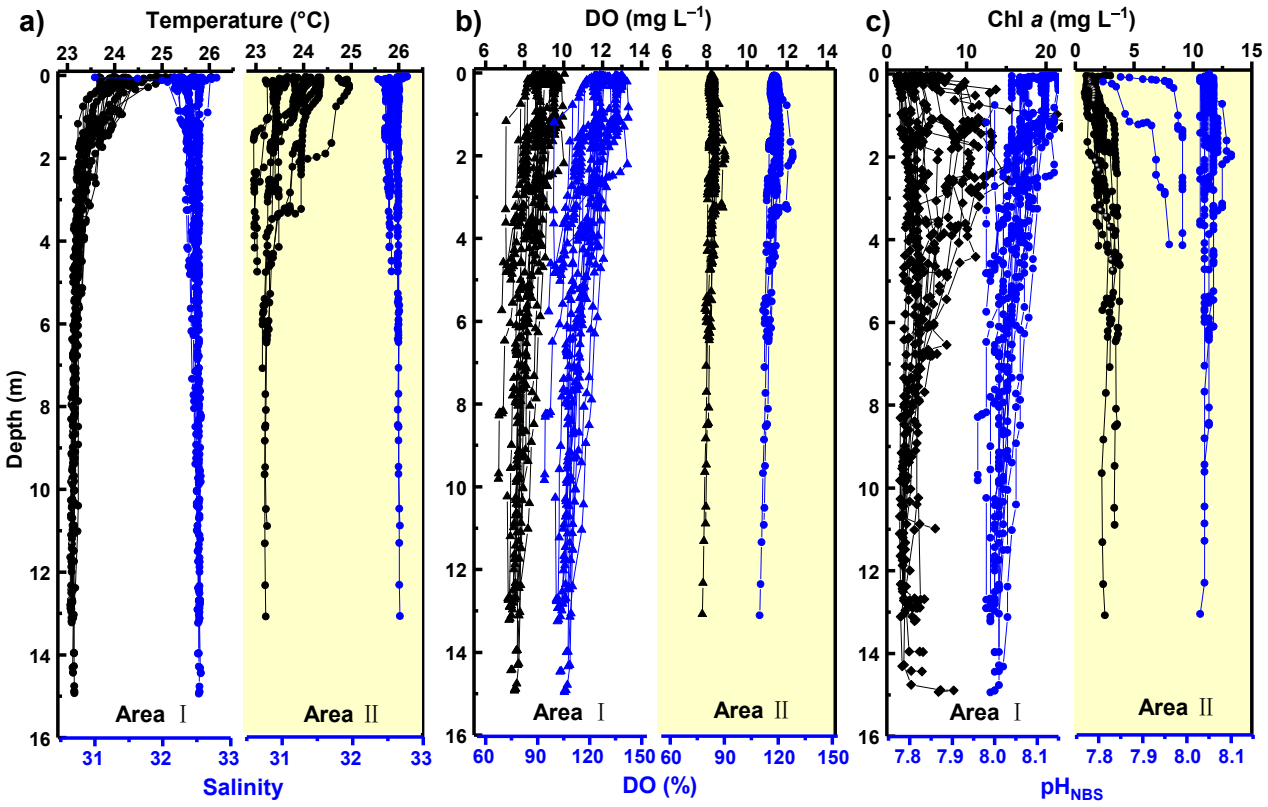

Figure A1. Distribution characteristics of temperature and salinity (**a**), DO (**b**), Chl *a* and pH$_{NBS}$ (**c**) in Yangmeikeng Sea Area (Area I) and Dalu Bay (Area II).

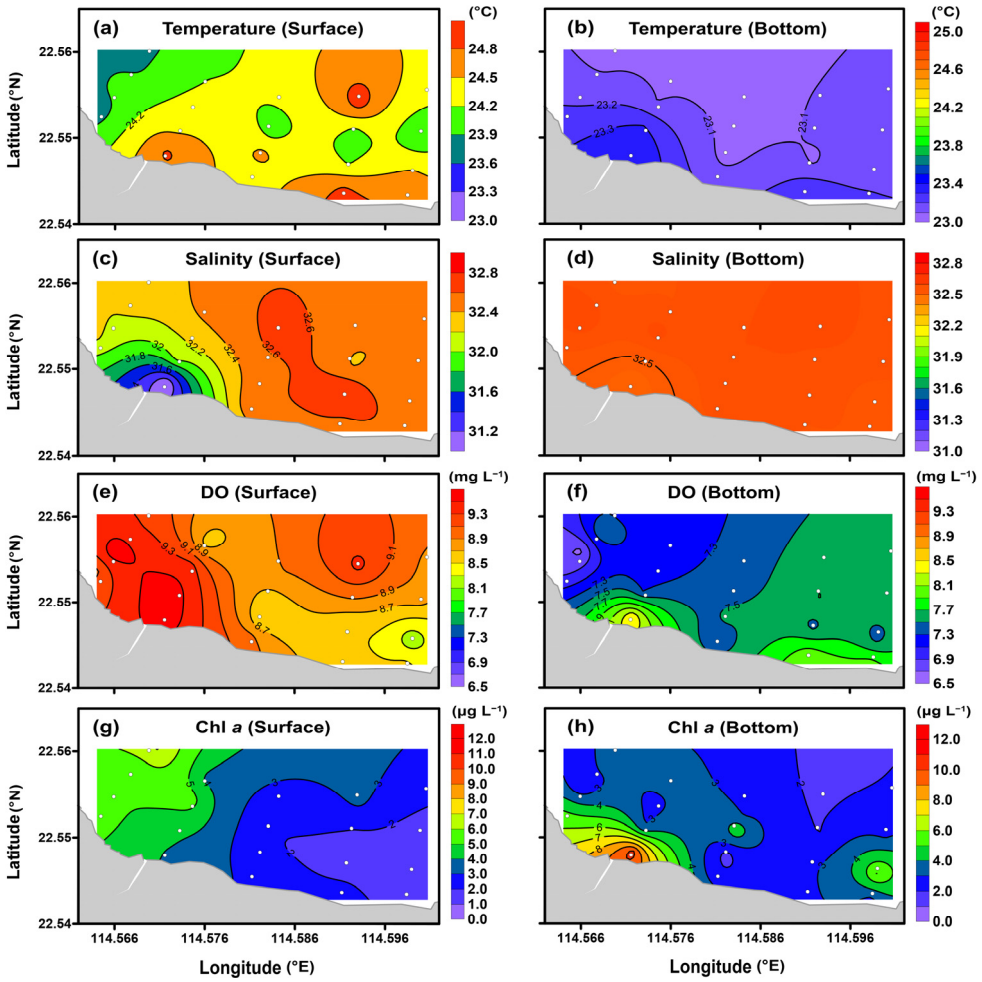

Figure A2. Distribution characteristics of temperature (**a**,**b**), salinity (**c**,**d**), DO (**e**,**f**) and Chl *a* (**g**,**h**) in the surface and bottom water of Yangmeikeng Sea Area (Area I).

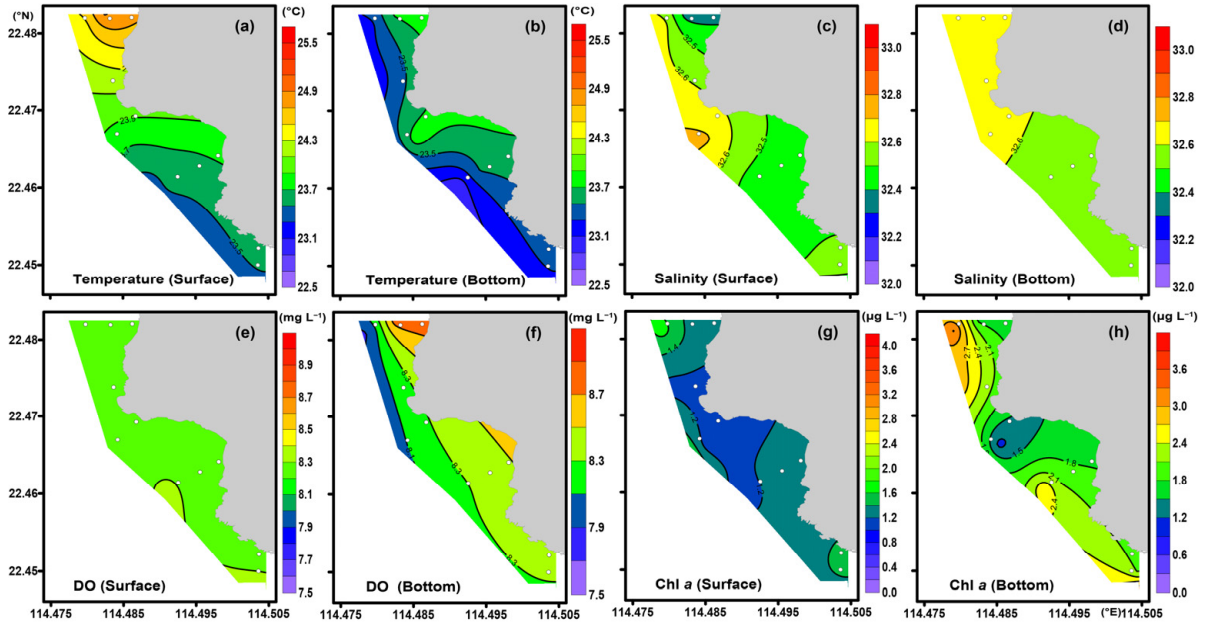

Figure A3. Distribution characteristics of temperature (**a**,**b**), salinity (**c**,**d**), DO (**e**,**f**) and Chl *a* (**g**,**h**), in the surface and bottom water of Dalu Bay (Area II).

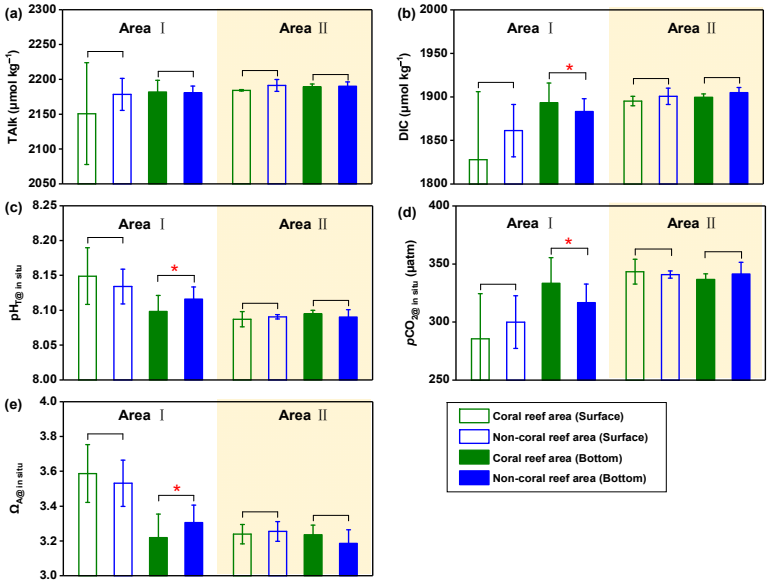

Figure A4. Averaged survey values (mean ± SD) of TAlk (**a**), DIC (**b**), $pH_{T@\ in\ situ}$ (**c**), $pCO_{2@\ in\ situ}$ (**d**) and $\Omega_{A@\ in\ situ}$ (**e**) in the surface and bottom water of Yangmeikeng Sea Area (Area I) and Dalu Bay (Area II). The significance at $p < 0.05$ was marked with *.

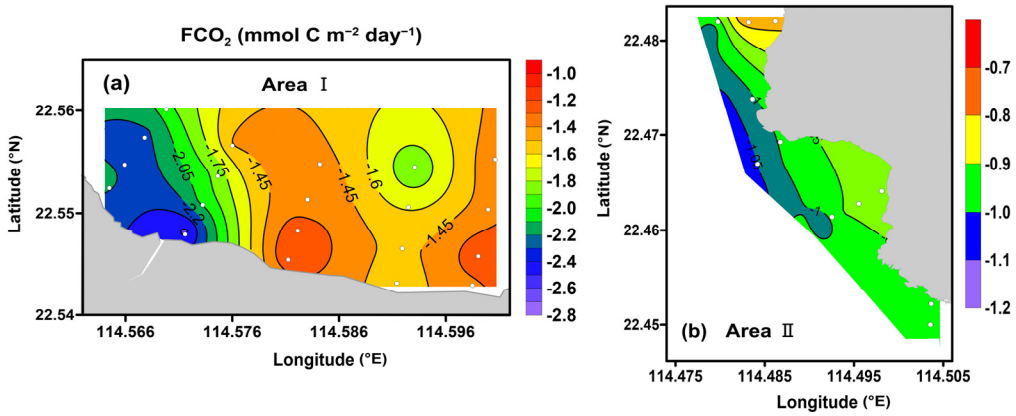

Figure A5. The air–sea fluxes of CO_2 (FCO_2, mmol m^{-2} day^{-1}) of Yangmeikeng Sea Area (Area I) (**a**) and Dalu Bay (Area II) (**b**).

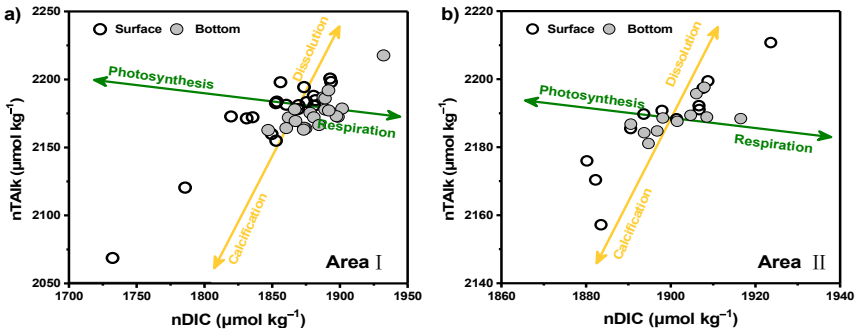

Figure A6. The nTAlk versus nDIC in the surface and bottom water of Yangmeikeng Sea Area (Area I) (**a**) and Dalu Bay (Area II) (**b**). Vectors illustrate the directions of the effects of photosynthesis, respiration and calcification on TAlk and DIC. The data of Area I (n = 42) and Area II (n = 22) were normalized to salinity of 32.44 and 32.57, respectively.

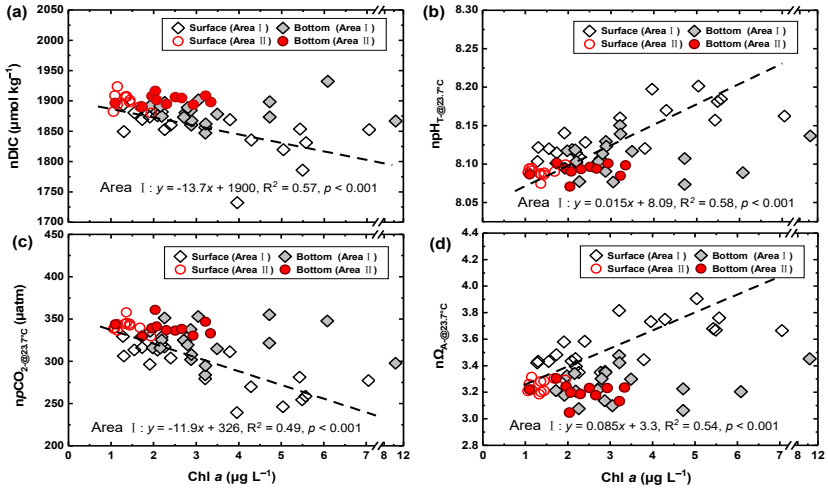

Figure A7. The correlation of carbonate parameters with Chl *a* (**a**–**d**) in the surface and bottom water of Yangmeikeng Sea Area (Area I) and Dalu Bay (Area II).

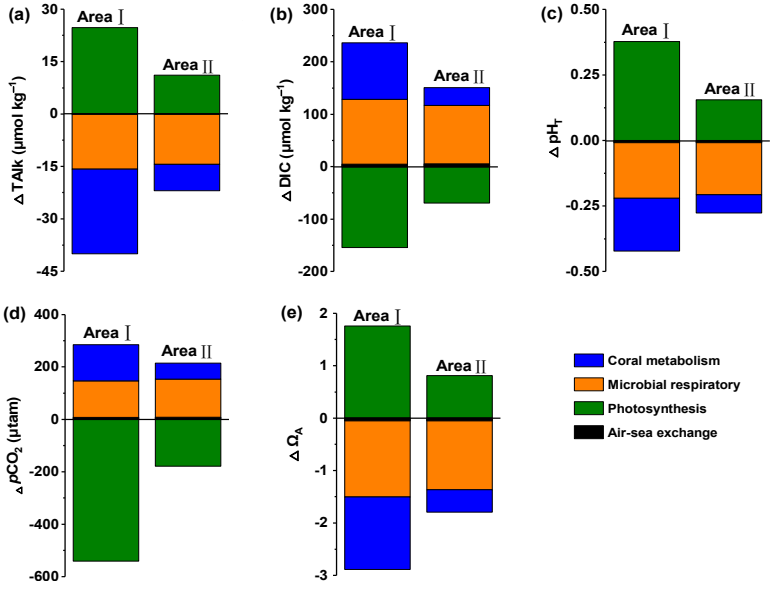

Figure A8. The contribution of photosynthesis, microbial respiration, coral metabolism and air–sea exchange to inorganic carbon dynamics (**a**–**e**) of the reef area of Yangmeikeng Sea Area (Area I) and Dalu Bay (Area II) in the in November.

References

1. NOAA. Trends in Atmosphere Carbon Dioxide, Global Greenhouse Gas Reference Network. 2022. Available online: https://www.esrl.noaa.gov/gmd/ccgg/trends/global.html (accessed on 28 November 2022).
2. Feely, R.A.; Sabine, C.L.; Lee, K.; Berelson, W.; Kleypas, J.; Fabry, V.J. Impact of anthropogenic CO_2 on the $CaCO_3$ system in the oceans. *Science* **2004**, *305*, 362–366. [CrossRef]
3. Le Quéré, C.; Andrew, R.M.; Friedlingstein, P.; Sitch, S.; Pongratz, J.; Manning, A.C.; Korsbakken, J.I.; Peters, G.P.; Canadell, J.G.; Jackson, R.B.; et al. Global carbon budget 2017. *Earth Syst. Sci. Data* **2018**, *10*, 405–448. [CrossRef]
4. Hamilton, S.L.; Kashef, N.S.; Stafford, D.M.; Mattiasen, E.G.; Kapphahn, L.A.; Logan, C.A. Ocean acidification and hypoxia can have opposite effects on rockfish otolith growth. *J. Exp. Mar. Biol. Ecol.* **2019**, *521*, 151245. [CrossRef]
5. Lee, Y.H.; Jeong, C.B.; Wang, M.; Hagiwara, A.; Lee, J.S. Transgenerational acclimation to changes in ocean acidification in marine invertebrates. *Mar. Pollut. Bull.* **2020**, *153*, 111006. [CrossRef] [PubMed]
6. Yang, B.; Gao, X.; Zhao, J.; Liu, Y.; Lui, H.K.; Huang, T.H.; Chen, T.; Xing, Q. Massive shellfish farming might accelerate coastal acidification: A case study on carbonate system dynamics in a bay scallop (*Argopecten irradians*) farming area, North Yellow Sea. *Sci. Total Environ.* **2021**, *798*, 149214. [CrossRef] [PubMed]

7. Fabry, V.J.; Seibel, B.A.; Feely, R.A.; Orr, J.C. Impacts of ocean acidification on marine fauna and ecosystem processes. *ICES J. Mar. Sci.* **2008**, *65*, 414–432. [CrossRef]
8. Wachs, T.D. The distribution of dissolved organic carbon in the Western Indian Ocean. *Deep. Sea Res. Oceanogr. Abstr.* **1964**, *11*, 757–765.
9. Winn, C.D.; Li, Y.H.; Mackenzie, F.T.; Karl, D.M. Rising surface ocean dissolved inorganic carbon at the Hawaii Ocean Time-series site. *Mar. Chem.* **1998**, *60*, 33–47. [CrossRef]
10. Bienson, C.V.; Wendy, A.; Michael, Y. Inorganic carbon utilization of tropical calcifying macroalgae and the impacts of intensive mariculture-derived coastal acidification on the physiological performance of the rhodolith *Sporolithon* sp. *Environ. Pollut.* **2020**, *266*, 115344.
11. Kerr, D.E.; Brown, P.J.; Grey, A.; Kelleher, B.P. The influence of organic alkalinity on the carbonate system in coastal waters. *Mar. Chem.* **2021**, *237*, 104050. [CrossRef]
12. Cai, W.J.; Hu, X.; Huang, W.J.; Murrell, M.C.; Lehrter, J.C.; Lohrenz, S.E. Acidification of subsurface coastal waters enhanced by eutrophication. *Nat. Geosci.* **2011**, *4*, 766–770. [CrossRef]
13. Chen, C.T.A.; Borges, A.V. Reconciling opposing views on carbon cycling in the coastal ocean: Continental shelves as sinks and near-shore ecosystems as sources of atmospheric CO_2. *Deep-Sea Res. II Top. Stud. Oceanogr.* **2009**, *56*, 578–590. [CrossRef]
14. Lonborg, C.; Calleja, M.L.; Fabricius, K.E.; Smith, J.N.; Achterberg, E.P. The great barrier reef: A source of CO_2 to the atmosphere. *Mar. Chem.* **2019**, *210*, 24–33. [CrossRef]
15. Cai, W.J.; Dai, M.; Wang, Y. Air-sea exchange of carbon dioxide in ocean margins: A province-based synthesis. *Geophys. Res. Lett.* **2006**, *33*, 347–366. [CrossRef]
16. Ries, J.B.; Ghazaleh, M.N.; Connolly, B.; Westfield, I.; Castillo, K.D. Impacts of seawater saturation state (Ω_A = 0.4–4.6) and temperature (10, 25 °C) on the dissolution kinetics of whole-shell biogenic carbonates. *Geochim. Cosmochim. Ac.* **2016**, *192*, 318–337. [CrossRef]
17. Ferrera, C.M.; Jacinto, G.S.; Chen, C.T.A.; Diego-Mcglone, M.L.S.; Datoc, M.F.K.T.; Lagumen, M.C.T. Carbonate parameters in high and low productivity areas of the Sulu Sea, Philippines. *Mar. Chem.* **2017**, *195*, 2–14. [CrossRef]
18. Dai, M.; Lu, Z.; Zhai, W.; Chen, B.; Cao, Z.; Zhou, K.; Cai, W.; Arthur, C.T. Diurnal variations of surface seawater pCO_2 in contrasting coastal environments. *Anglais* **2009**, *54*, 735–745. [CrossRef]
19. Xue, L.; Cai, W.J.; Sutton, A.J.; Sabine, C. Sea surface aragonite saturation state variations and control mechanisms at the Gray's Reef time-series site off Georgia, USA (2006–2007). *Mar. Chem.* **2017**, *195*, 27–40. [CrossRef]
20. Zhai, W.D.; Zhao, H.D.; Su, J.L.; Liu, P.F.; Li, Y.W.; Zheng, N. Emergence of summertime hypoxia and concurrent carbonate mineral suppression in the central Bohai Sea, China. *J. Geophys. Res-Biogeo.* **2019**, *124*, 2768–2785. [CrossRef]
21. Pipko, I.; Pugach, S.; Luchin, V.; Francis, O.; Savelieva, N.; Charkin, A. Surface CO_2 system dynamics in the Gulf of Anadyr during the open water season. *Cont. Shelf Res.* **2021**, *217*, 104371. [CrossRef]
22. Gobler, C.J.; DePasquale, E.L.; Griffith, A.W.; Baumann, H. Hypoxia and acidification have additive and synergistic negative effects on the growth, survival, and metamorphosis of early life stage bivalves. *PLoS ONE* **2014**, *9*, e83648. [CrossRef]
23. Tribollet, A.; Langdon, C.; Golubic, S.; Atkinson, M. Endolithic microflora are major primary producers in dead carbonate substrates of Hawaiian coral reefs. *J. Phycol.* **2006**, *42*, 292–303. [CrossRef]
24. Bates, N.R.; Astor, Y.M.; Church, M.J.; Currie, K.; Dore, J.E.; González-Dávila, M. A time-series view of changing surface ocean chemistry due to ocean uptake of anthropogenic CO_2 and ocean acidification. *Oceanography* **2014**, *27*, 126–141. [CrossRef]
25. Cotovicz, L.C., Jr.; Vidal, L.O.; de Rezende, C.E.; Bernardes, M.C.; Knoppers, B.A.; Sobrinho, R.L.; Abril, G. Carbon dioxide sources and sinks in the delta of the Paraíba do Sul River (Southeastern Brazil) modulated by carbonate thermodynamics, gas exchange and ecosystem metabolism during estuarine mixing. *Mar. Chem.* **2020**, *226*, 103869. [CrossRef]
26. Hannan, K.D.; Miller, G.M.; Watson, S.A.; Rummer, J.L.; Fabricius, K.; Munday, P.L. Diel pCO_2 variation among coral reefs and microhabitats at Lizard Island, Great Barrier Reef. *Coral Reefs* **2020**, *39*, 1391–1406. [CrossRef]
27. Yang, W.; Guo, X.; Cao, Z.; Xu, Y.; Wang, L.; Guo, L.; Dai, M. Seasonal dynamics of the carbonate system under complex circulation schemes on a large continental shelf: The northern South China Sea. *Prog. Oceanogr.* **2021**, *197*, 102630. [CrossRef]
28. Chauvaud, L.; Thompson, J.K.; Cloern, J.E.; Thouzeau, G. Clams as CO_2 generators: The *Potamocorbula amurensis* example in San Francisco Bay. *Limnol. Oceanogr.* **2003**, *48*, 2086–2092. [CrossRef]
29. Li, J.Q.; Zhang, W.W.; Ding, J.K.; Xue, S.Y.; Huo, E.Z.; Ma, Z.F. Effect of large-scale kelp and bivalve farming on seawater carbonate system variations in the semi-enclosed Sanggou Bay. *Sci. Total Environ.* **2021**, *753*, 142065. [CrossRef]
30. Choi, Y.; Kim, D.; Noh, J.H.; Kang, D.J. Contribution of Changjiang River discharge to CO_2 uptake capacity of the northern East China Sea in August 2016. *Cont. Shelf Res.* **2021**, *215*, 104336. [CrossRef]
31. Xu, X.; Zheng, N.; Zan, K. Aragonite saturation state variation and control in the river-dominated marginal BoHai and Yellow seas of China during summer. *Mar. Pollut. Bull.* **2018**, *135*, 540–550. [CrossRef]
32. Suzuki, A.; Kawahata, H. Carbon budget of coral reef systems: An overview of observations in fringing reefs, barrier reefs and atolls in the indo-Pacific region. *Tellus* **2003**, *55B*, 428–444. [CrossRef]
33. Borges, A.V.; Delille, B.; Frankignoulle, M. Budgeting sinks and sources of CO_2 in the coastal ocean: Diversity of ecosystems counts. *Geophys. Res. Lett.* **2005**, *32*, L14601. [CrossRef]
34. Cyronak, T.; Andersson, A.J.; Langdon, C.; Albright, R.; Bates, N. Taking the metabolic pulse of the world's coral reefs. *PLoS ONE* **2018**, *13*, e0190872. [CrossRef] [PubMed]

35. Yan, H.; Yu, K.; Shi, Q.; Tan, Y.; Zhang, H.; Zhao, M.; Li, S.; Chen, T.; Huang, L.; Wang, P. Coral reef ecosystems in the South China Sea as a source of atmospheric CO_2 in summer. *Chin. Sci. Bull.* **2011**, *56*, 676–684. [CrossRef]
36. Yan, H.; Yu, K.; Shi, Q.; Tan, Y.; Liu, G.; Zhao, M.; Li, S.; Chen, T.; Wang, Y. Seasonal variations of seawater pCO_2 and sea-air CO_2 fluxes in a fringing coral reef, northern South China Sea. *J. Geophys. Res. Oceans.* **2016**, *121*, 998–1008. [CrossRef]
37. Yan, S.H.; Tao, L.I. Evaluation of water quality status of coastal water in Dapeng Bay, Shenzhen. *Environ. Sci. Surv.* **2019**, *38*, 83–87.
38. Jia, C.; Wang, J.; Tang, Z. Distribution of coral communities in eastern sea area of Shenzhen. *J. Fish.* **2020**, *42*, 590–597.
39. Zhao, Y.; Yu, S.L.; Zhai, X.H.; Zhou, K.; Chen, M.R.; Qiu, J.W. Urban coral communities and water quality parameters along the coasts of Guangdong Province, China. *Mar. Pollut. Bull.* **2022**, *180*, 113821. [CrossRef]
40. Qi, Y.; Chen, J.; Wang, Z.; Xu, N.; Wang, Y.; Shen, P.; Lu, S.; Hodgkiss, I.J. Some observations on harmful algal bloom (HAB) events along the coast of Guangdong, southern China in 1998. *Hydrobiologia* **2004**, *512*, 209–214. [CrossRef]
41. Chen, X.; Wang, K.; Zhang, Z.; Zeng, Y.; Zhang, Y.; O'Driscoll, K. An assessment of wind and wave climate as potential sources of renewable energy in the nearshore Shenzhen coastal zone of the South China Sea. *Energy* **2017**, *134*, 789–801. [CrossRef]
42. Song, J.T.; Bi, H.S.; Cai, Z.H.; Cheng, X.M.; He, Y.H. Early warning of Noctiluca scintillans blooms using in-situ plankton imaging system: An example from Dapeng Bay, P.R. China. *Ecol. Indic.* **2020**, *112*, 106123. [CrossRef]
43. Grasshoff, K.; Kremling, K.; Ehrhardt, M. *Methods of Seawater Analysis*, 3rd ed.; Wiley-VCH: Weinheim, Germany, 1999; p. 632.
44. García, H.E.; Gordon, L.I. Oxygen solubility in seawater: Better fitting equations. *Limnol. Oceanogr.* **1992**, *37*, 1307–1312. [CrossRef]
45. Dickson, A.G. Standard potential of the (AgCl(s) + 1/2H2 (g) = Ag(s) + HCl(aq)) cell and the dissociation constant of bisulfate ion in synthetic sea water from 273.15 to 318.15 K. *J. Chem. Thermodyn.* **1990**, *22*, 113–127. [CrossRef]
46. Cadée, G.; Hegeman, J. Primary production of phytoplankton in the Dutch Wadden Sea. *Neth. J. Sea Res.* **1974**, *8*, 260–291. [CrossRef]
47. Li, B.; Li, G.W.; Jin, Y.; Ma, Y.Q.; Bai, Y.Y.; Sun, S. Distribution of chlorophyll-a and primary productivity in Yantai Sishili Bay. *Prog. Fish. Sci.* **2012**, *33*, 19–23.
48. Dickson, A.G. An exact definition of total alkalinity and a procedure for the estimation of alkalinity and total inorganic carbon from titration data. *Deep-Sea Res. Pt. II* **1981**, *28*, 609–623. [CrossRef]
49. Pelletier, G.J.; Lewis, E.; Wallace, D.W.R. *CO2SYS.XLS: A Calculator for the CO_2 System in Seawater for Microsoft Excel/VBA (Version 24)*; Washington State Department of Ecology: Olympia, DC, USA, 2015.
50. Lueker, T.J.; Dickson, A.G.; Keeling, C.D. Ocean pCO_2 calculated from dissolved inorganic carbon, alkalinity, and equations for K1 and K2: Validation based on laboratory measurements of CO_2 in gas and seawater at equilibrium. *Mar. Chem.* **2000**, *70*, 105–119. [CrossRef]
51. Lee, K.; Kim, T.W.; Byrne, R.H.; Millero, F.J.; Feely, R.A.; Liu, Y.M. The universal ratio of boron to chlorinity for the North Pacific and North Atlantic oceans. *Geochim. Cosmochim. Ac.* **2010**, *74*, 1801–1811. [CrossRef]
52. Meng, L.; Huang, W.; Yang, E.G. High temperature bleaching events can increase thermal tolerance of Porites lutea in the Weizhou Island. *Haiyang Xuebao* **2022**, *44*, 87–96.
53. Weiss, R.F. Carbon dioxide in water and seawater: The solubility of a non-ideal gas. *Mar. Chem.* **1974**, *2*, 203–215. [CrossRef]
54. Wanninkhof, R. Relationship between wind speed and gas exchange over the ocean. *J. Geophys Res-Oceans* **1992**, *97*, 7373–7382. [CrossRef]
55. South China Sea and Adjacent Seas Data Center. 2022. Available online: http://ocean.geodata.cn (accessed on 25 November 2022).
56. Guo, X.; Wong, G.T. Carbonate chemistry in the northern South China Sea shelf-sea in June 2010. *Deep-Sea Res. PT II* **2015**, *117*, 119–130. [CrossRef]
57. Yan, H.; Yu, K.; Shi, Q.; Lin, Z.; Zhao, M.; Tao, S.; Zhang, H. Air-sea CO_2 fluxes and spatial distribution of seawater pCO_2 in Yongle Atoll, northern-central South China Sea. *Cont. Shelf Res.* **2018**, *165*, 71–77. [CrossRef]
58. Zhang, C.; Huang, H.; Ye, C.; Huang, L.; Li, X.; Lian, J.; Liu, S. Diurnal and seasonal variations of carbonate system parameters on Luhuitou fringing reef, Sanya Bay, Hainan Island, South China Sea. *Deep-Sea Res. Pt. II* **2013**, *96*, 65–74. [CrossRef]
59. Akhand, A.; Watanabe, K.; Chanda, A.; Tokoro, T.; Kuwae, T. Lateral carbon fluxes and CO_2 evasion from a subtropical mangrove-seagrass-coral continuum. *Sci. Total Environ.* **2020**, *752*, 142190. [CrossRef]
60. Zang, H.; Li, Y.; Xue, L.; Liu, X.; Zhang, L. The contribution of low temperature and biological activities to the CO_2 sink in Jiaozhou Bay during winter. *J. Marine Syst.* **2018**, *186*, 37–46. [CrossRef]
61. Xue, L.; Cai, W.J.; Hu, X.; Sabine, C.; Jones, S.; Sutton, A.J. Sea surface carbon dioxide at the Georgia time series site (2006–2007): Air-sea flux and controlling processes. *Prog. Oceanogr.* **2016**, *140*, 14–26. [CrossRef]
62. Zhai, W.; Chen, J.; Jin, H.; Li, H.; Liu, J.; He, X. Spring carbonate chemistry dynamics of surface waters in the Northern East China Sea: Water mixing, biological uptake of CO_2, and chemical buffering capacity. *J. Geophys Res-Oceans.* **2014**, *119*, 5638–5653. [CrossRef]
63. Luo, X.; Wei, H.; Liu, Z.; Zhao, L. Seasonal variability of air–sea CO_2 fluxes in the Yellow and East China Seas: A case study of continental shelf sea carbon cycle model. *Cont. Shelf Res.* **2015**, *107*, 69–78. [CrossRef]
64. Chen, C.T.A.; Wang, S.L.; Lu, X.X.; Zhang, S.R.; Lui, H.K.; Tseng, H.C.; Huang, H.I. Hydrogeochemistry and greenhouse gases of the Pearl River, its estuary and beyond. *Quatern. Int.* **2008**, *186*, 79–90. [CrossRef]
65. Friis, K.; Körtzinger, A.; Wallace, D.W. The salinity normalization of marine inorganic carbon chemistry data. *Geophys. Res. Lett.* **2003**, *30*, 1085. [CrossRef]

66. Benson, B.B.; Krause, D. The concentration and isotopic fractionation of oxygen dissolved in fresh water and seawater in equilibrium with the atmosphere. *Limnol. Oceanogr.* **1984**, *29*, 620–632. [CrossRef]
67. Redfield, A.C. The biological control of chemical factors in the environment. *Am. Sci.* **1958**, *46*, 230A; 205–221.
68. Maske, H.; Medrano, R.C.; Castro, A.T.; Mercado, A.J.; Jauregui, C.O.; Castro, G.G. Inorganic carbon and biological oceanography above a shallow oxygen minimum in the entrance to the Gulf of California in the Mexican Pacific. *Limnol. Oceanogr.* **2010**, *55*, 481–491. [CrossRef]
69. Chen, C.T.; Pytkowicz, R.M.; Olson, E.J. Evaluation of the calcium problem in the South Pacific. *Geochem. J.* **1982**, *16*, 1–10. [CrossRef]
70. Duarte, B.; Freitas, J.; Valentim, J.; Medeiros, J.P.; Costa, J.L.; Silva, H.; Caçador, I. Abiotic control modelling of salt marsh sediments respiratory CO_2 fluxes: Application to increasing temperature scenarios. *Ecol. Indic.* **2014**, *46*, 110–118. [CrossRef]
71. Fagan, K.E.; Mackenzie, F.T. Air–sea CO_2 exchange in a subtropical estuarine-coral reef system, Kaneohe Bay, Oahu, Hawaii. *Mar. Chem.* **2007**, *106*, 174–191. [CrossRef]
72. Dellisanti, W.; Tsang, R.H.; Ang, P., Jr.; Wu, J.; Wells, M.L.; Chan, L. A diver-portable respirometry system for in-situ short-term measurements of coral metabolic health and rates of calcification. *Front. Mar. Sci.* **2020**, *7*, 571451. [CrossRef]
73. Longhini, C.M.; Souza, M.; Silva, A.M. Net ecosystem production, calcification and CO2 fluxes on a reef flat in Northeastern Brazil. *Estuar. Coast. Shelf S.* **2015**, *166*, 13–23. [CrossRef]